

# Effect of temperature on fracture properties of an amorphous poly(ethylene terephthalate) (PET) film

A. ARKHIREYEVA, S. HASHEMI

School of Polymer Technology, University of North London, UK

E-mail: s.hashemi@unl.ac.uk

Fracture behaviour of an amorphous polyethylene terephthalate (PET) film with a glass transition temperature ( $T_g$ ) of 72°C and a thickness of 0.21 mm was studied between 23 and 70°C using Double Edge Notched Tension (DENT) specimens. Within this temperature range, DENT specimens fractured by ductile tearing of the ligament region after ligament region had been fully yielded. The load-displacement curves obtained for different ligament lengths were geometrically similar to one another. On the basis of these, *Essential Work of Fracture* (EWF) methodology was used to determine fracture toughness of the PET film as a function of temperature. A linear relationship was obtained between the total specific work of fracture,  $w_f$ , and ligament length,  $L$ , at temperatures under consideration. Results showed that specific essential work of fracture,  $w_e$ , is independent of temperature but the specific non-essential work of fracture ( $\beta w_p$ ) increases with increasing temperature and drops in value near the glass-transition temperature. A linear relationship was also found for yielding ( $w_y$ ) and necking/tearing ( $w_{nt}$ ) components of  $w_f$  as a function of ligament length. The specific essential work components were found to be temperature dependent and whilst component  $w_{ey}$  decreased component  $w_{ent}$  increased with increasing temperature. The contribution of  $w_{ent}$  to  $w_e$  was substantially greater than that of  $w_{ey}$  at all temperatures. © 2002 Kluwer Academic Publishers

## 1. Introduction

The linear elastic fracture mechanics (LEFM) approach is generally used to study fractures occurring at nominal stresses well below the yield stress of the material. Under this condition, the area in which energy is dissipated near the crack tip is so small that the entire specimen is assumed to exhibit Hookean elasticity. However, in characterising the failure of ductile materials, the LEFM approach becomes redundant mainly due to development of a large plastic zone at the crack tip. As a consequence of this, the energy dissipation is no longer confined to a small local zone near the crack tip.

For materials that show significant crack tip plasticity, other techniques such as the *J-integral* and the *Essential Work of Fracture* (EWF) must be used to quantify fracture toughness. Although the *J-integral* approach has been used traditionally for this purpose, the EWF method has gained popularity due to its experimental simplicity and used extensively to study fracture behaviour of wide range of polymeric materials [e.g., 1–20].

The present work applies the concept of EWF for characterising plane-stress ductile fracture of PET film of thickness 0.210 mm as a function of temperature. In addition, partitioning of the EWF into yielding and necking/tearing related terms is also considered and the

effect of temperatures on these terms is investigated. The PEN material used in this study is an amorphous material with a glass transition temperature of 72°C as indicated by the Differential Scanning Calorimeter (DSC) trace in Fig. 1.

## 2. Deformation behaviour

The uniaxial tensile yield stress ( $\sigma_y$ ) and modulus ( $E$ ) of the PET material was measured between 23 and 70°C in an Instron testing machine at a constant crosshead speed of 5 mm/min, using dumbbell-shaped specimens having constant width of 4 mm and length of 56 mm within the gauge length region.

The tensile load-displacement ( $P$ - $\delta$ ) curves, typical examples of which are presented in Fig. 2 show that within the temperature range selected for this study, failure of the PET specimens occurred after extensive amount of plastic deformation. It can be seen from Fig. 2 that load-displacement diagrams show a clear yield point (maximum load) and a drop in load after yield owing to strain softening (shear band formation). A sudden rise in load was then registered (except at 70°C) and followed by a region of cold drawing (drawing of the necked region) during which tensile deformation continued at a constant stress level until failure point was reached.

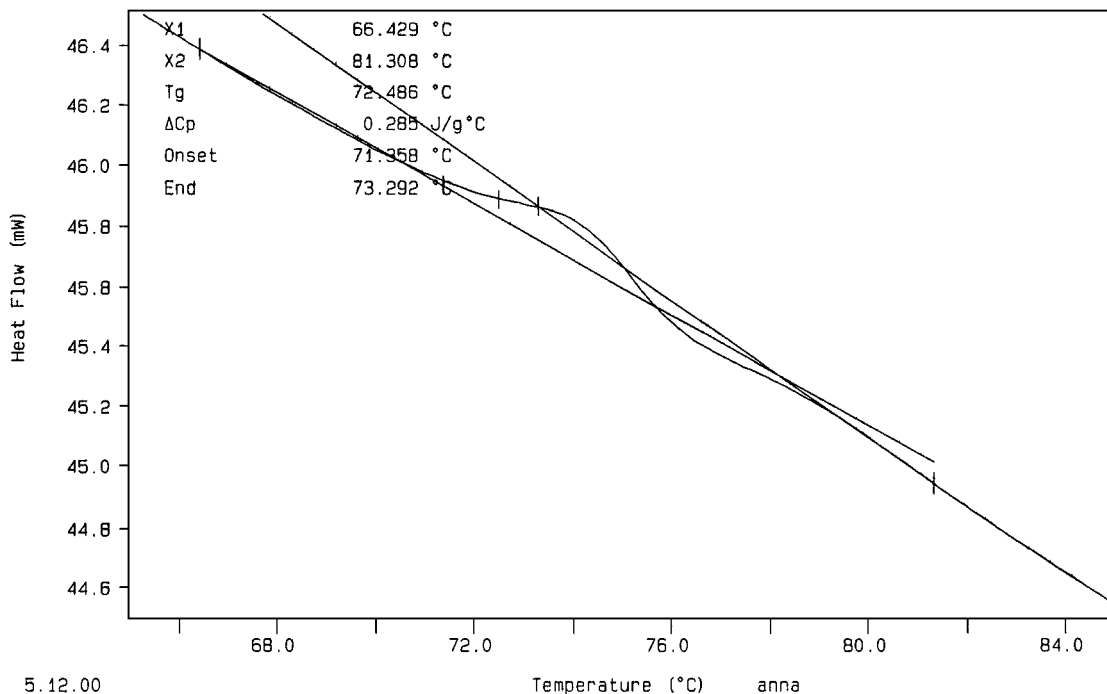


Figure 1 DSC trace for PET.

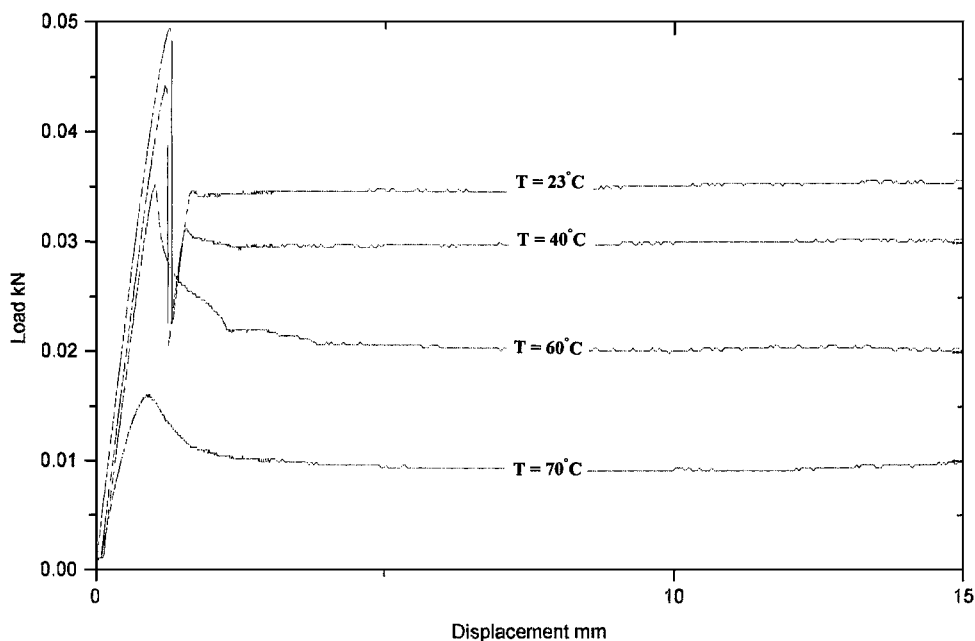


Figure 2 Tensile load-displacement curve *s* at different testing temperatures.

Results obtained from tensile tests are summarised in Table I where it can be seen that tensile yield stress ( $\sigma_y$ ) and modulus ( $E$ ) both decreased with increasing temperature as expected, owing to the temperature dependence of the viscoelastic response of the material.

### 3. Fracture behaviour

To study the effect of temperature on fracture behaviour of PET film, rectangular coupons with a width ( $W$ ) of 35 mm and length ( $H$ ) of 70 mm were cut from A4 size sheets having nominal thickness ( $B$ ) of 0.210 mm. The coupons were then notched to produce series of Double-Edge Notched Tension (DENT) specimens as shown in Fig. 3a with ligament length ( $L$ ) in the range of 3 to 15 mm. To ensure the two notches

were aligned, a line was drawn across the width of the specimen at its mid-point prior to notching. After notching, DENT specimens were tested to complete failure in an Instron testing machine using pneumatic clamps with an initial separation ( $Z$ ) of 35 mm. The fracture tests were performed at a constant crosshead displacement rate of 5 mm/min between 23°C and 70°C. The load-displacement ( $P$ - $\delta$ ) curve for each specimen was recorded using a computer data logger.

The DENT load-displacement curves in Fig. 4 indicate that failure of the DENT specimens closely resembles that of tensile specimens (see Fig. 2). It can be seen from the curves in Fig. 4 that the length of the ligament region had no major influence on the fracture behaviour of the PET film. As ligament length increased, so did

TABLE I Summary of the fracture data at different temperatures

Fracture parameters	$T = 23^{\circ}\text{C}$	$T = 40^{\circ}\text{C}$	$T = 60^{\circ}\text{C}$	$T = 70^{\circ}\text{C}$
$\sigma_y$ (MPa)	63	55	44	33
$E$ (GPa)	3.11	3.05	2.96	1.87
$w_e$ (kJ/m <sup>2</sup> )	81	80	80	82
$w_{ey}$ (kJ/m <sup>2</sup> )	16	11	9	7
$w_{ent}$ (kJ/m <sup>2</sup> )	65	68	72	75
$\beta w_p$ (MJ/m <sup>3</sup> )	10.7	11.3	11.1	10
$\beta_y w_{py}$ (MJ/m <sup>3</sup> )	0.79	0.60	0.23	0.10
$\beta_{nt} w_{pnt}$ (MJ/m <sup>3</sup> )	9.9	10.7	10.9	9.9
$\beta$	0.07	0.09	0.11	–
$w_p$ (MJ/m <sup>3</sup> )	147	126	101	–
$2R_p$ (mm)	20	25	41	45
$e_b$ (mm)	1.9	2.1	2.7	3.2
$e_p$	0.49	0.63	0.77	1.20
$w_e$ (kJ/m <sup>2</sup> ) ( $\lambda = 1.15$ )	134	133	135	121
$w_e$ (kJ/m <sup>2</sup> ) ( $\lambda = 0.67$ )	78	77	78	70
$w_e$ (kJ/m <sup>2</sup> ) ( $\lambda = 0.77$ )	90	89	90	81

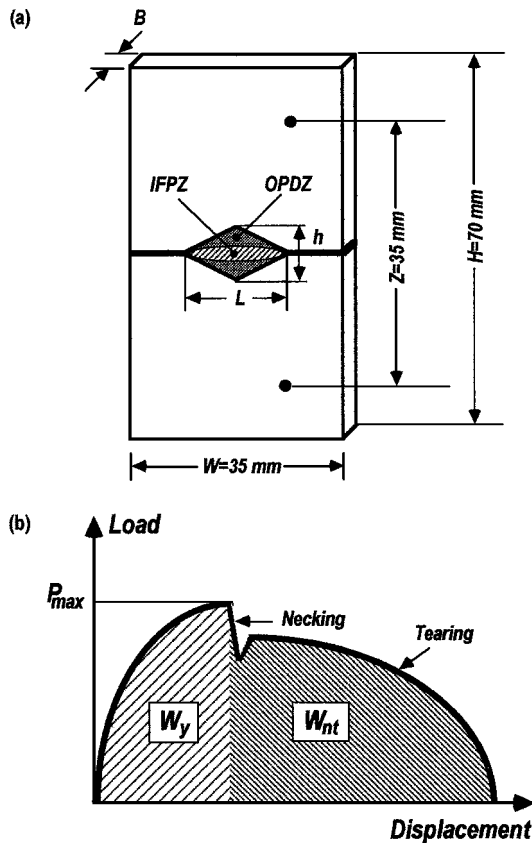


Figure 3 (a) Double edge notched tension specimen. (b) Partitioning of the total work of fracture,  $W_f$ .

the area under the curve, the maximum load and the extension at break. However, whilst maximum load decreased, extension at break increased with increasing temperature.

The visual observation of the specimens during the tests and the general behaviour of the load-displacement curves in Fig. 4 were both indicative of a failure that involves extensive crack tip yielding and slow crack growth. The sequence of events that led to the final fracture of the DENT specimens can be described as:

- (i) Opening and blunting of the initial crack.
- (ii) Development of a duckbill-shaped plastic zone at each crack tip.

- (iii) Full-yielding of the ligament length region.
- (iv) Ductile tearing of the ligament region and the eventual failure of the test specimen.

It was noted that at maximum load, the two plastic zones met mid-way along the ligament region. At this point, plastic zones overlapped and ligament region necked down giving rise to a very prominent load-drop after maximum. However, in the temperature range between  $23^{\circ}\text{C}$  and  $60^{\circ}\text{C}$ , this load drop was not sufficient to tear the whole ligament and therefore to maintain tearing of the ligament region, the load had to increase again before decreasing towards zero.

Fig. 5 shows typical examples of the fractured specimens as a function of test temperature. It is notable that at  $70^{\circ}\text{C}$ , the boundary of the plastic deformation zone can not be clearly defined as test temperature approaches the glass transition temperature of the material (i.e.,  $T_g = 70^{\circ}\text{C}$ ). The DENT specimens tested above  $T_g$  did not show any evidence of crack propagation.

#### 4. Fracture toughness evaluation

To assess fracture toughness, test data were analysed using the *Essential Work of Fracture* (EWF) methodology. This method was used for two reasons; (i) the geometric similarity during crack growth existed between specimens of different ligament lengths, as revealed by the load-displacement curves in Fig. 4, and (ii) the ligament length had been fully yielded prior to crack initiation.

The EWF concept was first proposed by Broberg [21] who suggested that when failure of the test specimen is preceded by extensive yielding and slow crack growth, as in this study, a toughness parameter called *Specific Essential Work of Fracture*,  $w_e$  can be evaluated. It has been shown that the specific essential work of fracture ( $w_e$ ) is a material constant for given thickness representing the work required for crack initiation or, as the case may be, crack propagation.

According to EWF, the non-elastic region at the tip of crack may be divided into two regions as illustrated in Fig. 3a—An inner fracture process zone (IFPZ) and an outer plastic deformation zone (OPDZ). The total work of fracture,  $W_f$ , can then be partitioned into two components, i.e.,

$$W_f = W_e + W_p \quad (1)$$

The term  $W_e$  is the work expended in the IFPZ to form a neck and its subsequent tearing and the term  $W_p$  is the work dissipated in the OPDZ where various types of deformation such as shear yielding and microvoiding may be operating.

The work  $W_e$  is termed *Essential Work of Fracture* (EWF). It is essentially a surface energy term whose value under plane-stress conditions is proportional to the ligament area ( $LB$ ), i.e.,

$$W_e = w_e BL \quad (2)$$

The work  $W_p$  in Equation 1 is termed the *Non-Essential Work of Fracture*. It is assumed that under plane-stress

conditions,  $W_p$  is proportional to the volume of the yielded zone ( $BL^2$ ), i.e.,

$$W_p = w_p \beta BL^2 \quad (3)$$

where  $w_p$  is the plastic work done per unit volume and  $\beta$  is a proportionality constant or shape factor associated with the volume of the plastic deformation zone. Introducing Equations 2 and 3 into Equation 1 gives:

$$w_f = \frac{W_f}{LB} = w_e + \beta w_p L \quad (4)$$

where  $w_f$  is termed the *Specific Work of Fracture*.

Equation 4 suggests  $w_f$  is a linear function of ligament length,  $L$ . The specific essential work of fracture,  $w_e$ , is given by the positive intercept at  $L=0$  of the linear regression interpolating the data and the specific non-essential work of fracture,  $\beta w_p$ , is given by the slope of the regression line.

Since DENT load-displacement curves for PET showed a prominent load drop after maximum, it was considered worthwhile to partition  $W_f$  into two components as shown in Fig. 3b:

(i) Work required for complete *yielding* of the ligament length region,  $W_y$

(ii) Work required for *necking/tearing* of the ligament region,  $W_{nt}$   
i.e.,

$$W_f = W_y + W_{nt} \quad (5)$$

Previous studies [8, 9, 12, 14] have shown that when  $W_f$  is partitioned in this way, variation of the specific work terms  $w_y$  and  $w_{nt}$  with  $L$  follows that of  $w_f$  with  $L$ . Equation 4 was then split into:

$$w_y = \frac{W_y}{LB} = w_{ey} + \beta_y w_{py} L \quad (6)$$

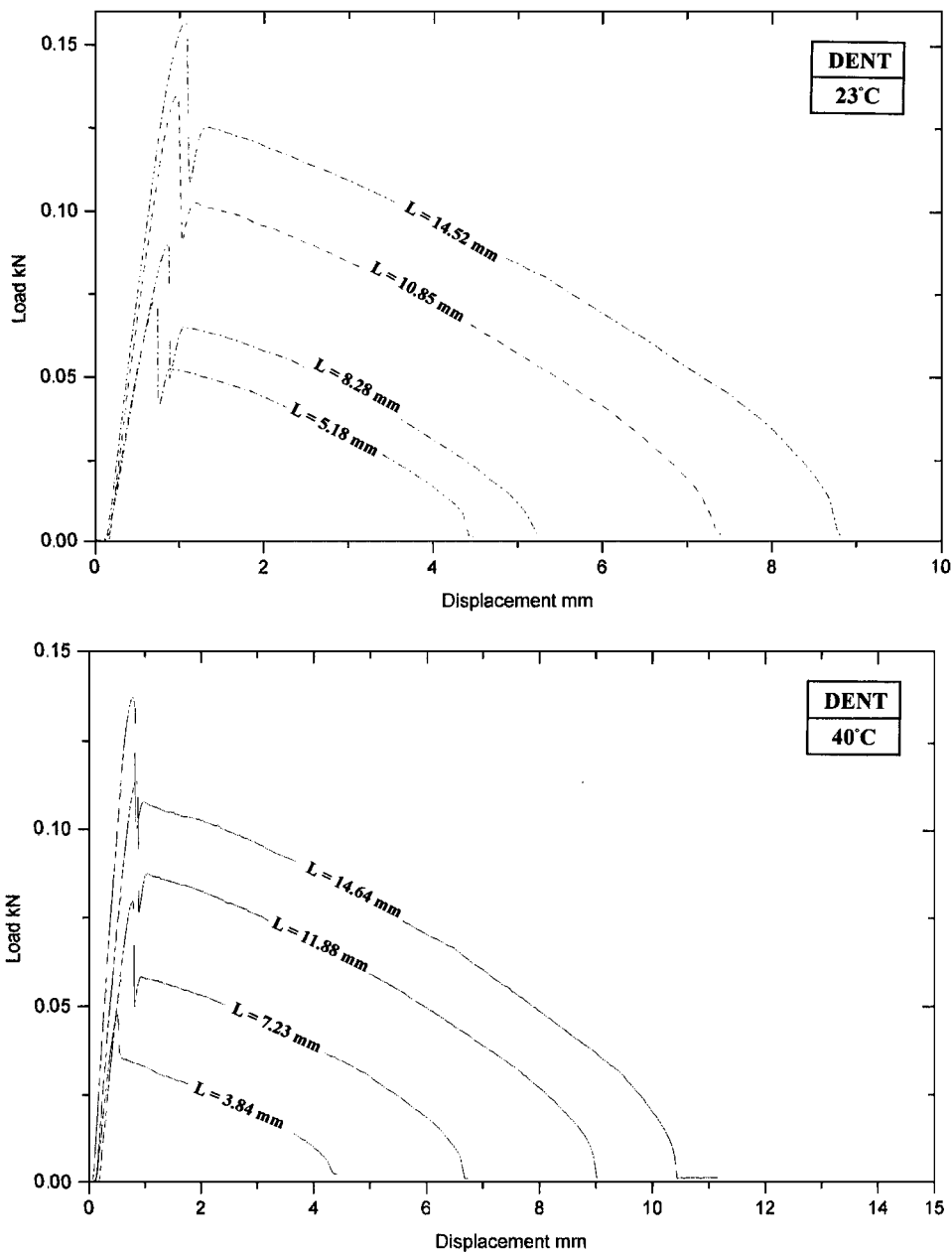


Figure 4 Typical DENT load-displacement curves at various ligament lengths as a function of test temperature. (Continued.)

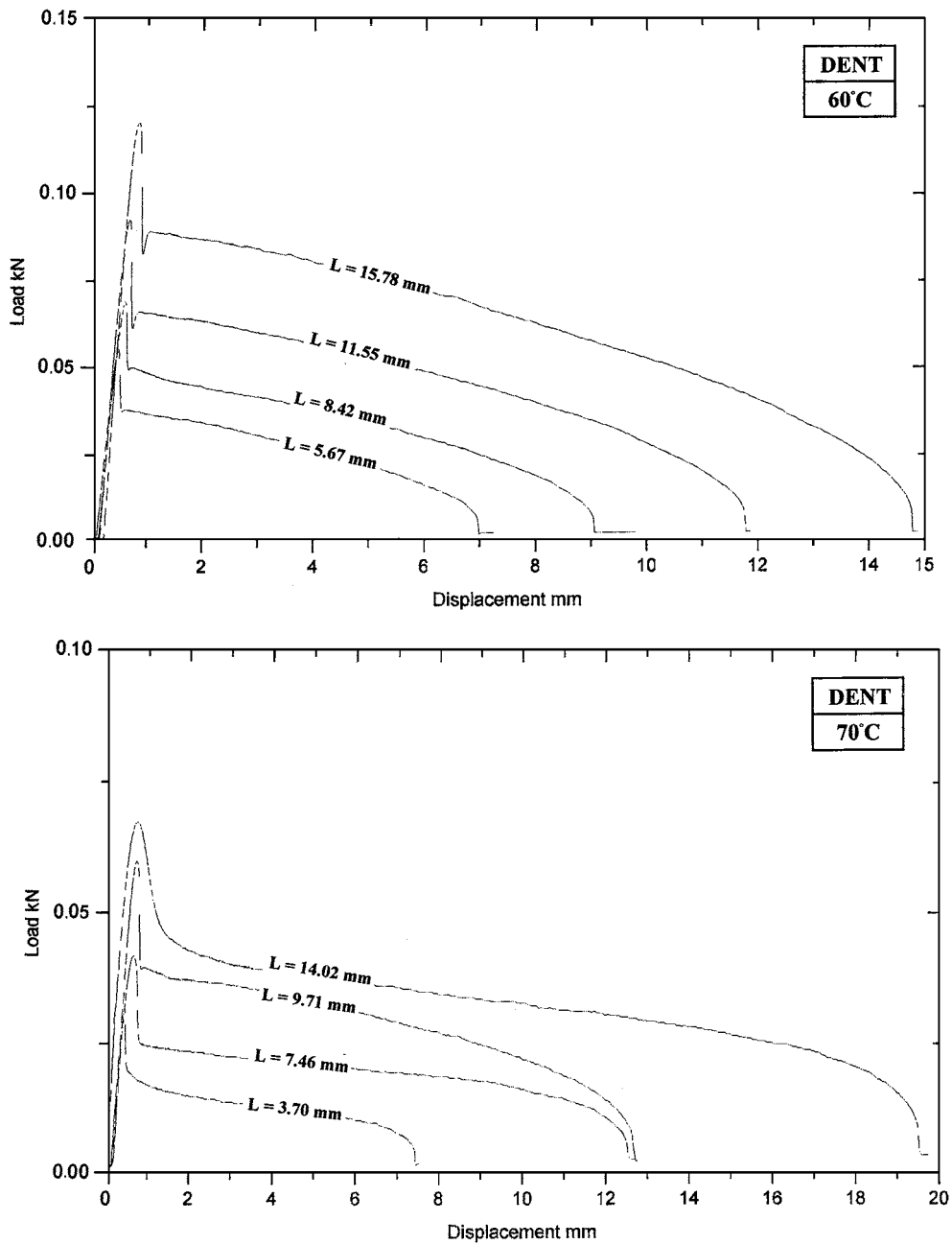


Figure 4 (Continued.)

$$w_{nt} = \frac{W_{nt}}{LB} = w_{ent} + \beta_{nt} w_{pnt} L \quad (7)$$

The terms  $w_{ey}$  and  $w_{ent}$  represent the yielding and the necking/tearing components of the specific essential work of fracture respectively i.e.,

$$w_e = w_{ey} + w_{ent} \quad (8)$$

The terms  $\beta_y w_{py}$  and  $\beta_{nt} w_{pnt}$  represent the yielding and the necking/tearing components of the specific non-essential work of fracture respectively, i.e.,

$$\beta w_p = \beta_y w_{py} + \beta_{nt} w_{pnt} \quad (9)$$

Fig. 6a–d shows plots of the specific work of fracture parameters ( $w_f$ ,  $w_{nt}$  and  $w_y$ ) versus ligament length between 23 and 70°C. It can be seen that within this temperature range, specific work terms are linearly depen-

dent upon ligament length as suggested by Equations 4, 6 and 7. It is evident from these plots that the amount of work contributing to  $w_f$  by each component varies with test temperature. It is realised that whilst  $w_y$  decreases,  $w_{nt}$  increases, with increasing temperature. As clearly demonstrated in Fig. 6a–d  $w_y$  is always smaller than  $w_{nt}$ . This is also apparent from the load-displacement curves in Fig. 4, where it can be seen that extension at maximum load is very small compared to that at break. Consequently, a greater proportion of the specific work of fracture ( $w_f$ ) stems from the necking/tearing part of the fracture process rather than its yielding part.

To determine values of specific essential and non-essential work of fracture parameters, the best linear regression line was drawn through each set of data in Fig. 6. The intercept values at zero ligament length (i.e.,  $w_e$ ,  $w_{ent}$  and  $w_{ey}$ ) and the slope of the lines (i.e.,  $\beta w_p$ ,  $\beta_y w_{py}$  and  $\beta_{nt} w_{pnt}$ ) are given in Table I and plotted as a function of temperature in Fig. 7a and b.

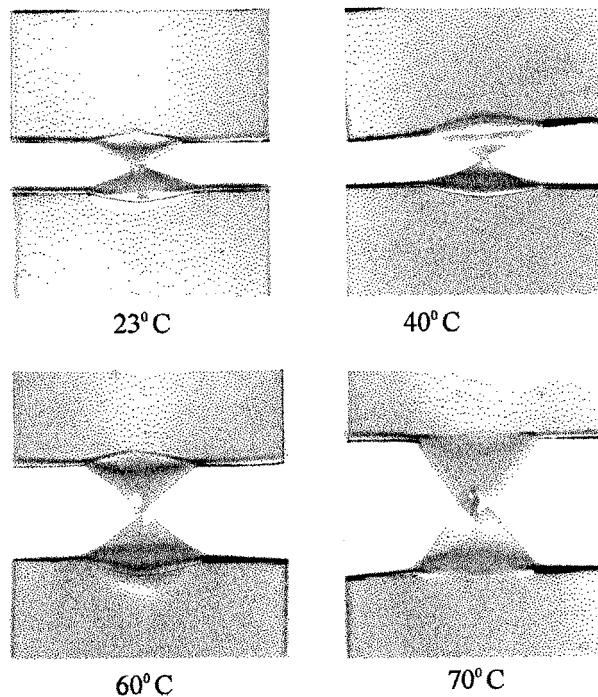


Figure 5 Typical DENT fractured specimens at different temperatures.

According to Fig. 7a,  $w_e$  is independent of temperature but its components  $w_{ey}$  and  $w_{ent}$  both change with temperature. It can be seen that whilst  $w_{ey}$  decreases,  $w_{ent}$  increases with increasing temperature. Clearly,  $w_{ent}$  term is substantially greater than  $w_{ey}$  term at all temperatures. It can be deduced that at 23°C approximately 80% of  $w_e$  is contributed by the necking/tearing

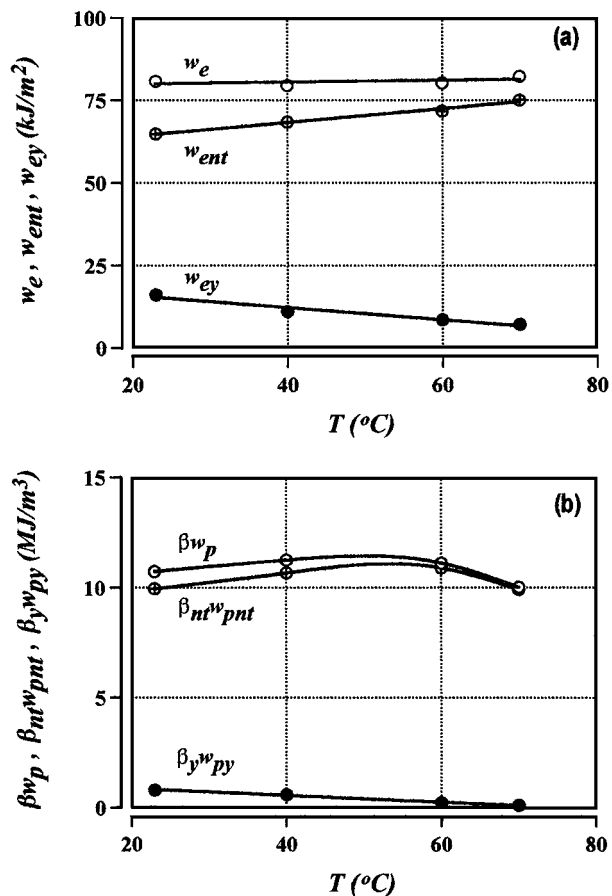


Figure 7 (a) Specific essential work of fracture parameters versus temperature. (b) Specific non-essential work of fracture parameters versus temperature.

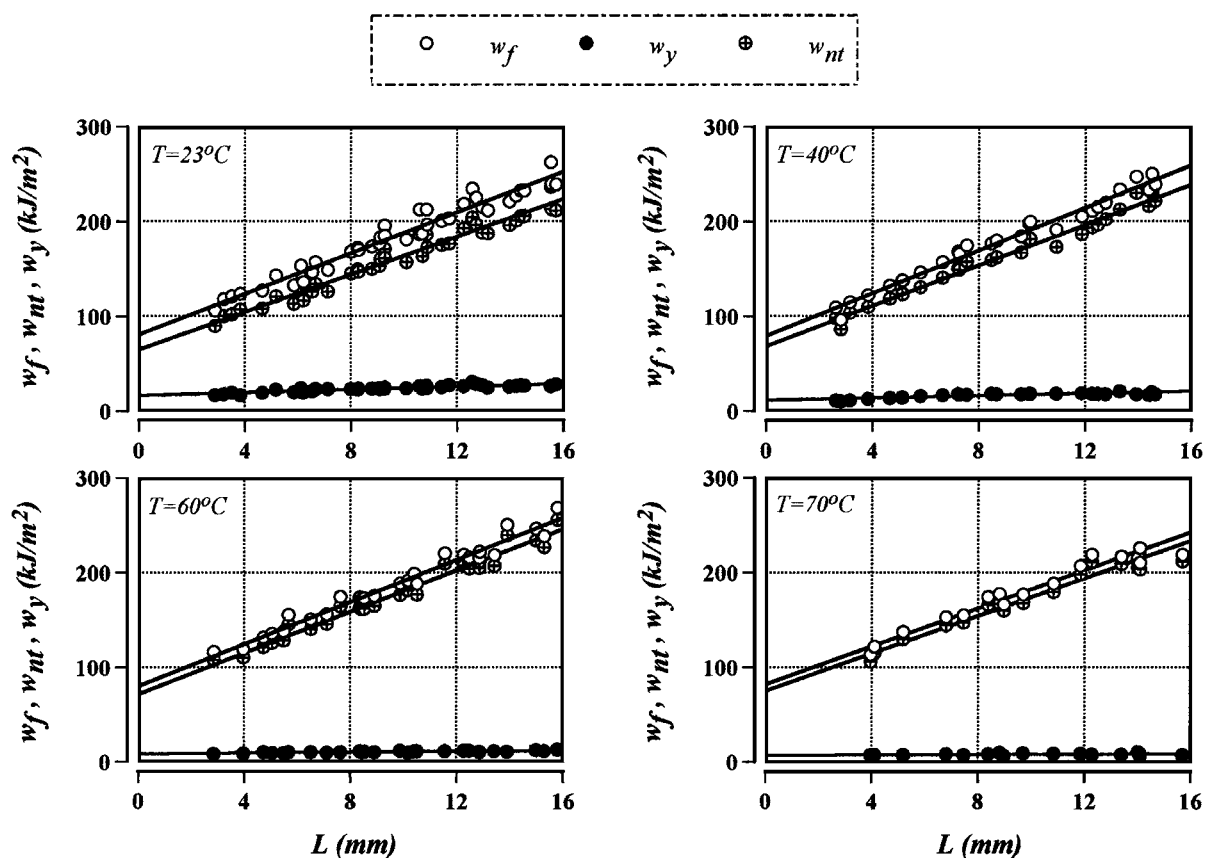


Figure 6 Specific work of fracture parameters versus ligament length at different temperatures.

component whereas at 70°C, this value rises to approximately 93%.

It is worth noting that since crack initiation occurred at maximum load, values of  $w_{ey}$  reported in this study can be regarded as specific essential work of fracture for crack initiation.

As regards non-essential work terms, it can be seen from Fig. 7b, that  $\beta w_p$  and its component  $\beta_{nt} w_{pnt}$ , both increase with temperature and decrease in the vicinity of the glass transition temperature. In contrast,  $\beta_y w_{py}$  component decreases with increasing temperature over the whole temperature range under consideration. Evidently,  $\beta_y w_{py}$  decreases linearly with temperature, predicting that  $\beta_y w_{py} = 0$  at 76°C. Specimens tested around this temperature showed no evidence of cracking. It is worth noting, that since  $\beta_y w_{py}$  contribution to  $\beta w_p$  is very small compared to that of  $\beta_{nt} w_{pnt}$ , variation of  $\beta w_p$  term with temperature closely resembles that of  $\beta_{nt} w_{pnt}$  with temperature.

To determine the value of the plastic work per unit volume,  $w_p$ , height of the plastic deformation zone,  $h$ , was measured as a function of ligament length. For a diamond shaped plastic deformation zone of height,  $h$  (see Fig. 3a) and volume  $V_p(L, B)$ , we have;

$$V_p(L, B) = BLh/2 = \beta BL^2 \quad (10)$$

giving a linear relationship between  $h$  and  $L$ , with slope of  $2\beta$ , i.e.,

$$h = 2\beta L \quad (11)$$

Fig. 8a shows plots of  $h$  versus  $L$  between 23°C and 60°C. It can be seen, as suggested by Equation 11, variation at any given temperature is linear over the entire ligament length range under consideration. Values of  $\beta$  derived from the slope of the lines in Fig. 8a are plotted as a function of temperature in Fig. 8b where it can be seen that  $\beta$  increases linearly with increasing temperature. It is worth noting that linear extrapolation of the line in Fig. 8b suggests that  $\beta = 0$  at  $-50^\circ\text{C}$ . This suggests that the plastic flow in the ligament region becomes very negligible and a horizontal line is obtained when  $w_f$  is plotted against  $L$ . This means that  $w_f = w_e$  at  $-50^\circ\text{C}$  and therefore a brittle fracture is expected for PET.

Values of plastic work per unit volume ( $w_p$ ) are given in Table I and as expected they decrease with increasing temperature as shown in Table I.

## 5. Validity of the EWF measurements

Although the linearity of the plots in Figs 6a and 8a implies that EWF measurements reported in this work relate to plane-stress fracture and therefore valid, it is nonetheless interesting to examine the validity of the measurements in terms of conditions imposed on the length of the ligament region.

It has been proposed that for valid measurements of plane-stress  $w_e$ , the ligament length has to satisfy the following pre-requisites [e.g., 22]:

$$3B - 5B \leq L \leq \min\left(\frac{W}{3}, 2R_p\right) \quad (12)$$

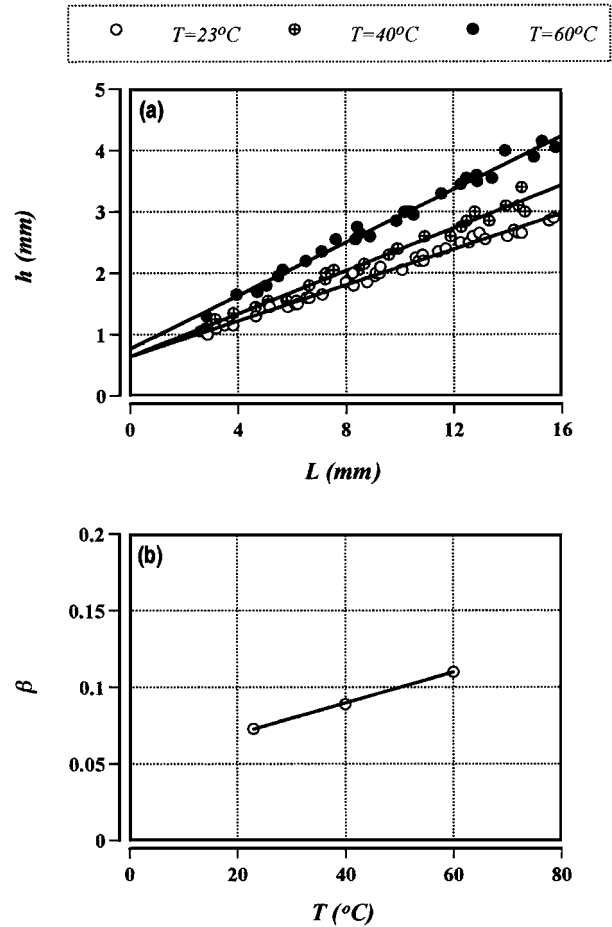


Figure 8 (a) Height of the plastic deformation zone versus ligament length at different temperatures. (b) Plastic zone shape factor versus temperature.

where  $2R_p$  is the size of the plastic deformation zone give by:

$$2R_p = \frac{E w_e}{\pi \sigma_y^2} \quad (13)$$

According to Equation 12, to maintain the state of pure plane-stress in the ligament region, the smallest ligament length value ( $L_{\min}$ ) for EWF testing should be greater than three to five times the specimen thickness. For the case in which  $L < L_{\min}$ , the state of stress in the ligament region becomes one of mixed mode (i.e., having both plane-stress and plane-strain characteristics) in which case the linear relation between  $w_f$  and  $L$  may not be valid and the stress state become pure plane strain as  $L$  approaches zero. Realising that in the mixed-mode region  $w_e = w_e(L, B)$ —but that  $\beta w_p$  is invariant with  $L$ , Mai and Cotterell [1] proposed that the plane-strain specific essential work of fracture ( $w_{Ie}$ ) can be obtained by linear extrapolation of  $w_f$  in the mixed-mode region (region B in Fig. 9a) to a ligament length of zero. Saleemi and Nairn [2] later developed a modified methodology in which they determined that  $w_e(L, B) = (w_f - \beta w_p L)$  and plotted it against ligament length. This gave a straight line that on extrapolating to  $L = 0$  yielded the plane-strain specific essential work of fracture,  $w_e(0, B) = w_{Ie}$ .

According to the pre-requisite  $L_{\min} = 3B - 5B$ , for thickness value of 0.21 mm, the length of the ligament

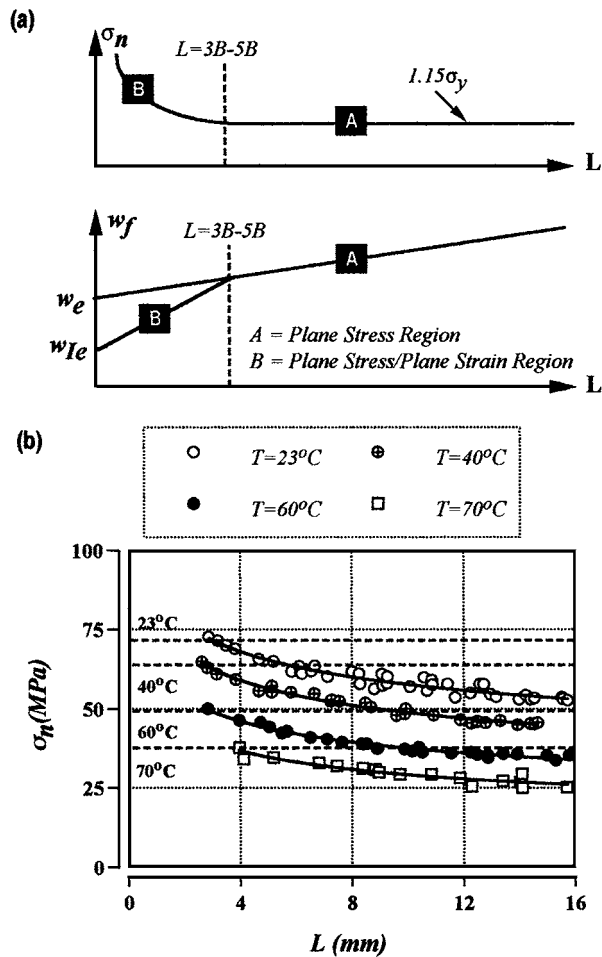


Figure 9 (a) Schematics representation of net-section stress and specific work of fracture versus ligament length. (b) Net-section stress versus ligament length at different temperatures.

region should be greater than 1.05 mm to ensure plane-stress fracture, which of-course has been through out this study.

Another indication of the type of stress state in the ligament region is the way in which net-section stress ( $\sigma_n$ ) at maximum load varies with ligament length. According to analysis by Hill [23], in the plane-stress region,  $\sigma_n$  becomes independent of ligament length and for DENT type specimens attains a value of  $1.15\sigma_y$ , where  $\sigma_y$  is the uniaxial tensile yield stress of the material. In the mixed mode region however,  $\sigma_n$  increases with shortening of the ligament length region as plastic constraint effect rises. As shown schematically in Fig. 9a, this increase in  $\sigma_n$  often leads to a decrease in the  $w_f$  value.

The effect of ligament length on  $\sigma_n$  at all four temperatures is shown in Fig. 9b where it can be seen that  $\sigma_n$  decreases with increasing  $L$ . Although it is difficult to locate precisely at what ligament length stress-state transition occurs, tentatively it seems that this transition occurs at a ligament length value of  $\approx 6-8$  mm, in which case,  $L/B$  ratio at transition point is  $\approx 35$  and not 3 to 5, as recommended. However, bearing in mind that  $w_f-L$  and  $h-L$  plots were reasonably linear even for ligament lengths less than 6 mm, the observed variation in  $\sigma_n$  with  $L$  may well be due to factors other than the transition in stress-state. Moreover, given that values of  $\sigma_n$  are consistently lower than the  $1.15\sigma_y$  (shown

as broken line in Fig. 9b), the likelihood of plane-stress failure outweighs that of the mixed mode type failure. If failure of specimens was indeed under mixed mode conditions, then the implications are that either the requirements  $3B-5B$  is not sufficient to guarantee plane-stress conditions or that increases in constraint factor were small enough not to affect the plots.

As for the condition  $L \leq \min(W/3, 2R_p)$ , this is prescribed for two reasons. Firstly, to ensure that the size of the OPDZ is not disturbed by the edge effect; hence the pre-requisite  $L \leq W/3$ . Secondly, to ensure that complete yielding of the ligament region occurs before crack growth thereby the proportionality of  $W_p$  and  $L^2$  is maintained; hence, the pre-requisite  $L \leq 2R_p$ . The plastic zone size values,  $2R_p$ , calculated using Equation 13 are given in Table I. It can be seen that  $2R_p$  is greater than  $W/3$  ( $\approx 11.67$  mm) at all test temperatures and therefore the upper threshold value for  $L$  is determined by the length  $W/3$ . However, pre-requisite  $L \leq W/3$  plays no significant role in this study as plots of  $w_f$  versus  $L$  and  $h$  versus  $L$ , remained linear for all values of  $L$  tested here.

## 6. Crack opening displacement (COD)

Estimation of  $w_e$  via COD has received a considerable attention by several investigators [e.g., 5, 10, 12, 14, 20, 22]. This estimation has been derived from a simple relationship

$$w_e = \lambda\sigma_y COD \quad (14)$$

where  $\sigma_y$  is the tensile yield stress and  $\lambda$  is a constant. Although Equation 14 has been used with some success, in its application, values of  $\lambda$  ranging from 1.15 to 0.67 have been used where  $\lambda = 1.15$  takes into account notch constraint effect (i.e.,  $\lambda\sigma_y = \sigma_n$ ) and  $\lambda = 0.67$  assumes a parabolic shape for the load-displacement curves.

The crack opening displacement can be obtained by plotting the extension at break,  $e_b$ , versus ligament length. It has been shown [e.g., 5, 10, 12, 14, 20, 22] that variation of  $e_b$  with  $L$  conforms to a straight-line relationship of the form:

$$e_b = e_o + e_p L \quad (15)$$

where  $e_o$  is the intercept value of  $e_b$  at zero ligament length representing the COD of the advancing crack tip and  $e_p$  is the plastic contribution to extension.

Fig. 10a shows the variation of  $e_b$  with ligament length as a function of temperature. It can be seen that  $e_b$  increases linearly with ligament length at all temperatures. The intercept values at zero ligament length,  $e_o$ , are plotted as a function of temperature in Fig. 10b, where it can be seen that it increases with increasing temperature. A similar observation can be made for  $e_p$  (see Table I).

Table I gives estimated values of  $w_e$  for  $\lambda = 1.15$ , 0.67 and 0.77, where the latter takes into account notch constraint effect as well assuming a parabolic shape load-displacement curves. It can be seen that by and large  $\lambda = 0.67$  and 0.77 provide a reasonable estimation of  $w_e$ . This suggests that there is competition between yield stress and crack opening displacement



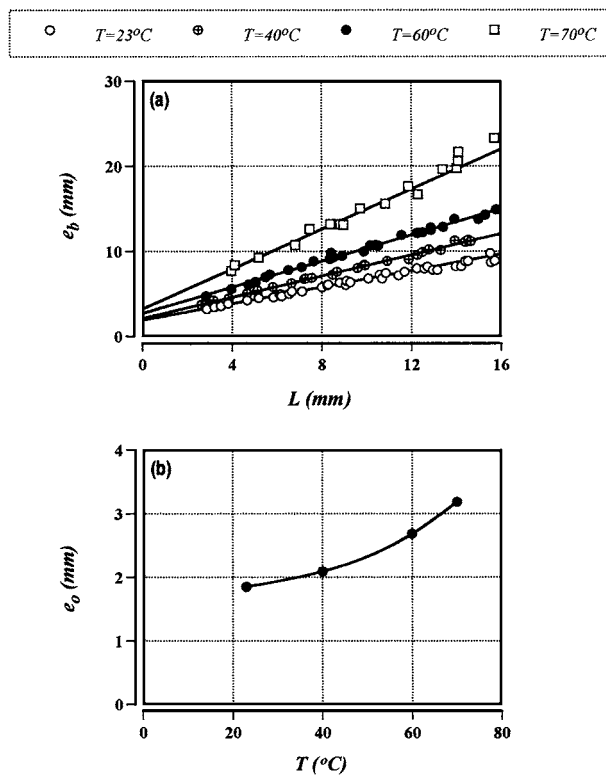


Figure 10 (a) Extension to break versus ligament length at different temperature. (b) Crack opening displacement versus temperature.

values, which determines  $w_e$ , and its dependence on the temperature.

## 7. Conclusions

The effect of temperature on plane-stress ductile fracture behaviour of an amorphous polyethylene terephthalate film of thickness 0.210 mm was studied by the essential work of fracture method using double edge notched specimens.

Results indicated that the specific essential work of fracture,  $w_e$ , is independent of temperature between 23 $^\circ\text{C}$  and 70 $^\circ\text{C}$ . It was found that when  $w_f$  is partitioned into yielding and necking/tearing components, a linear relationship is obtained for each component with respect to ligament length. The specific essential fracture works for yielding ( $w_{ey}$ ) and for necking/tearing ( $w_{ent}$ ) were found temperature dependent, the latter increased and whereas the former decreased with increasing temperature over the entire temperature range under consideration. Moreover, it was found that the contribution made to  $w_e$  by  $w_{ent}$  was substantially greater than that made by  $w_{ey}$ .

The specific non-essential work of fracture,  $\beta w_p$ , and its components linked to yielding ( $\beta_y w_{py}$ ) and necking/tearing ( $\beta_{nt} w_{pnt}$ ) were temperature dependent. Results showed that  $\beta_{nt} w_{pnt}$  is much greater than  $\beta_y w_{py}$ . This suggested that the plastic zone development in PET is linked mostly to the necking/tearing processes. A linear relationship was also obtained between the height of the plastic deformation zone ( $h$ ) and ligament length below  $T_g$ . The plastic zone shape factor ( $\beta$ ) increased with temperature whilst the plastic work done per unit volume ( $w_p$ ) decreased. Analysis further demonstrated that there is competition between values of the crack opening displacement and yield stress, which determines the  $w_e$  value and its variation with respect to temperature.

## References

1. Y. W. MAI and B. COTTERELL, *Int. J. Fract.* **32** (1986) 105.
2. A. S. SALEEMI and J. A. NARIN, *Polym. Eng. Sci.* **30** (1990) 211.
3. Y. W. MAI, B. COTTERELL, R. HORLYCK and G. VIGNA, *ibid.* **27** (1987) 804.
4. S. HASHEMI, *Plast. Rub. Comp. Proc. Appl.* **20** (1993) 229.
5. J. WU, Y. W. MAI and B. COTTERELL, *J. Mater. Sci.* **28** (1993) 3373.
6. W. Y. F. CHAN and J. G. WILLIAMS, *Polym.* **35** (1994) 1666.
7. J. WU and Y. W. MAI, *Polym. Eng. Sci.* **36** (1996) 2275.
8. J. KARGER-KOCSIS and T. CZIGANY, *Polym.* **37** (1996) 2433.
9. J. KARGER-KOCSIS, T. CZIGANY and E. J. MOSKALA, *ibid.* **38** (1997) 4587.
10. S. HASHEMI, *J. Mater. Sci.* **32** (1997) 1573.
11. J. KARGER-KOCSIS, T. CZIGANY and E. J. MOSKALA, *Polym.* **39** (1998) 3939.
12. A. ARKHIREYEVA, S. HASHEMI and M. O'BRIEN, *J. Mater. Sci.* **34** (1999) 5961.
13. J. J. CASELLAS, P. M. FRONTINI and J. M. CARELLA, *J. Appl. Polym. Sci.* **74** (1999) 781.
14. S. HASHEMI and J. G. WILLIAMS, *Plast. Rub. Compos.* **29** (2000) 294.
15. S. HASHEMI, *Polym. Eng. Sci.* **40** (2000) 132.
16. *Idem.*, *ibid.* **40** (2000) 798.
17. *Idem.*, *ibid.* **40** (2000) 1435.
18. E. C. Y. CHING, R. K. Y. LI and Y. W. MAI, *ibid.* **40** (2000) 310.
19. D. E. MOUZAKIS, J. KARGER-KOCSIS and E. J. MOSKALA, *J. Mater. Sci. Lett.* **19** (2000) 1615.
20. A. ARKHIREYEVA and S. HASHEMI, *Plast. Rub. Compos.* **30** (2001) 125.
21. K. B. BROBERG, *Int. J. Fract.* **4** (1968) 11.
22. J. G. WILLIAMS and A. PAVAN, "Fracture of Polymers, Composites and Adhesives" (Elsevier, Oxford, 2000).
23. R. H. HILL, *J. Mech. Phys. Solids* **1** (1952) 19.

Received 25 July 2001

and accepted 9 April 2002